arXiv:1305.0316v1 [cond-mat.mes-hall] 1 May 2013

Spin Caloritronics in graphene with Mn

Alberto Torres,[1, a)] Matheus P. Lima,[1, b)] A. Fazzio,[1, c)] and Antônio J. R. da Silva[1, 2, d)]
[1)] *Instituto de Física de Universidade de São Paulo, CP 66318, 05315-970, São Paulo, SP, Brazil.*
[2)] *Laboratório Nacional de Luz Síncrotron, CP 6192, 13083-970, Campinas, SP, Brazil.*

(Dated: 3 May 2013)

We show that a device made of graphene with Mn adatoms trapped at single vacancies feature spin-dependent Seebeck effect, thus enabling the use of this material for spin caloritronics applications. More than that, it is possible to tune its thermoelectric properties with a gate potential in a way the system presents either a nearly total spin polarized current, flowing in one given direction, or currents for both spins flowing in opposite directions without net charge transport.

PACS numbers: 72.20.Pa, 72.80.Vp, 85.75.-d, 72.25.Ba
Keywords: Seebeck effect, graphene, spin caloritronics, density functional theory, electronic transport

The field of spin caloritronics deals with the interaction of spin and heat currents, that is, the coupling between spintronics and thermoelectrics[1]. Graphene[2,3] is a potential candidate material for spintronic devices[4,5] due to its long mean free path and weak spin-orbit coupling. Furthermore, it has been shown that graphene has potential for thermoelectric applications, both theoretically[6,7] and experimentally[8–10]. Therefore, at least in principle, graphene is a good candidate for real applications in spin caloritronics. Devices made of graphene nanoribbons with zigzag edges have already been proposed to this end[11,12]. However, it is an experimentally difficult task to synthesize nanoribbons with well defined zigzag edges[13]. Bi-dimensional graphene itself, although a good conductor for spin polarized currents, is spin degenerate, so it cannot be used as a *source* for spin polarized currents. One way to lift its spin degeneracy that has been investigated recently is to dope graphene with metal adatoms[14–19]. Although their tendency is to diffuse and to form clusters, they can be trapped in defects like single vacancies (SV), where they are highly stable[15,20].

It has already been shown by some of us that Mn atoms trapped at SV (Mn@SV) in graphene are tightly bound (with a binding energy of −6.0 eV) and act as a source of spin polarized currents under a bias voltage. Moreover, these currents can be tuned by a gate potential[15], V_g. Being that so, it is natural to ask if the thermoelectric properties of this kind of device would also be spin dependent. In this work, we address this question by calculating the thermoelectric properties and currents of a device consisting of graphene with a Mn@SV under the effect of a gate voltage and with contacts held at different temperatures (see Fig. 1).

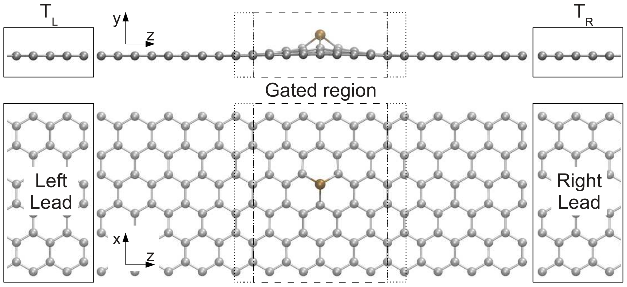

FIG. 1. (Color online) Schematic view of the geometry of the device studied, a graphene sheet (periodic in the x direction) with a Mn atom trapped at a single vacancy, coupled to pristine graphene contacts. The central region of the device is under the effect of gate potential.

Our calculations have been performed with nonequilibrium Green functions coupled to density functional theory (NEGF+DFT) in the linear regime. First, the geometries, comprised of a Mn@SV in a graphene supercell ($13.0 \times 20.0 \times 32.5$ Å^3), have been fully relaxed with a force criterion of 0.02 eV/Å using the SIESTA code[21]. Then, we calculated the transmittances using the TRANSAMPA2 code[22]. The electrodes were considered to be semi-infinite pristine graphene sheets. In all calculations we used the Perdew-Burke-Ernzerhof generalized gradient approximation[23] for the exchange-correlation functional, norm-conserving pseudopotentials[24] and a double-ζ polarized basis. We used an energy mesh cutoff of 300 Ry and a $7 \times 1 \times 4$ k-point sampling, in the Monkhorst-Pack[25] scheme, to integrate the Brillouin zone. For the electronic transport calculations we employed 101 $k_\perp$-points (x direction in Fig. 1). The gate potential was simulated by adding a smooth electrostatic potential to the Hamiltonian in a finite region (a xy slab) containing the Mn@SV in the self-consistent cycle, thus allowing screening effects by charge rearrangement[15]. This potential consisted of a plateau, $U(z) = eV_g$ for $z_0 < z < z_1$, represented by a dashed line in Fig. 1, with smooth sinusoidal steps with width τ, indicated by the dotted lines in Fig. 1. $U(z) = 0$ elsewhere. In the calculations we defined the gated region trough $z_0 = 11.24$ Å,

---

[a)] Electronic mail: atriera@if.usp.br
[b)] Electronic mail: mplima@if.usp.br
[c)] Electronic mail: fazzio@if.usp.br
[d)] Electronic mail: ajrsilva@if.usp.br

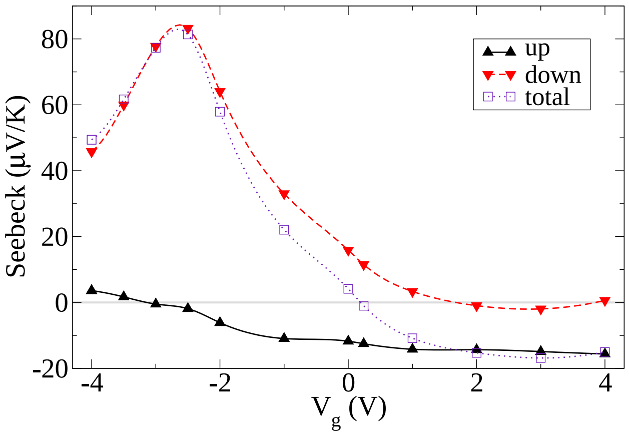

FIG. 2. (Color online) Seebeck coefficients for the up and down spin channels versus gate potential for an average temperature of 300 K. The lines are just guides to the eyes.

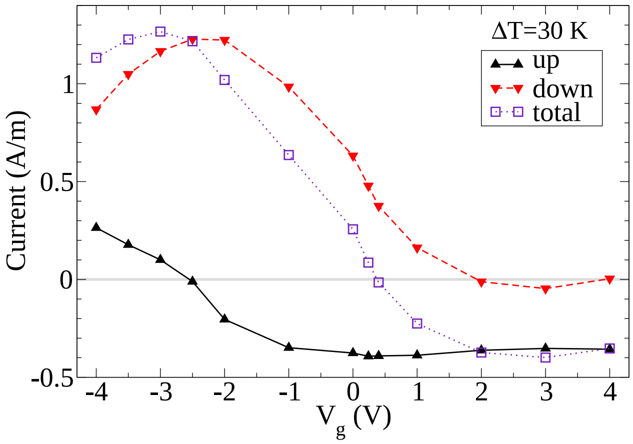

FIG. 3. (Color online) Current versus gate voltage, V_g, for a fixed temperature difference of $\Delta T = 30$ K (the left electrode is kept at room temperature, $T_L = 300$ K, and the right electrode at $T_R = 330$ K). The lines are just guides to the eyes.

$z_1 = 21.23$ Å and $\tau = 1.25$ Å. A vacuum layer of 20 Å was used to avoid spurious interactions between periodical images in the direction perpendicular to the graphene plane (y in Fig. 1).

In the Landauer-Büttiker formalism, the current is given by[26]

$$I_\sigma = \frac{e}{h} \int \mathcal{T}_\sigma(E; V_g)\,(f_L - f_R)\,(E - \mu)\,dE, \qquad (1)$$

where $\sigma = \uparrow, \downarrow$ is the spin, e is the electron charge, h is the Planck constant, $\mathcal{T}_\sigma(E; V_g)$ is the spin resolved transmittance function, which depends on the gate voltage V_g; $f_{L(R)} \equiv f(E, \mu, T_{L(R)})$ is the Fermi-Dirac distribution function, μ is the chemical potential of the electrodes and $T_{L(R)}$ is the temperature of the left(right) lead.

The Seebeck coefficient, also named thermoelectric power, is a measure of the voltage induced by a temperature difference on a device or material and is defined as $S = -\Delta V/\Delta T|_{I=0}$. In the limiting case of $\Delta V \to 0$ and $\Delta T \to 0$ (the linear regime) an expression for S can be derived from an expansion of Eq. (1), given by[27]

$$S_\sigma = -\frac{1}{e\overline{T}} \frac{\int \mathcal{T}_\sigma(E; V_g)\left(-\frac{\partial f}{\partial E}\right)(E - \mu)\,dE}{\int \mathcal{T}_\sigma(E; V_g)\left(-\frac{\partial f}{\partial E}\right)\,dE}, \qquad (2)$$

where $\overline{T}$ is the average temperature between the contacts.

In Fig. 2 we show the calculated Seebeck coefficients for the up and down spin channels as a function of V_g at room temperature ($\overline{T} = T_{L(R)} = 300$ K). Close to zero gate, around $V_g = 0.24$ V, where S_{tot} ($= S_\uparrow + S_\downarrow$) crosses 0 V/K; the system presents $S_\uparrow$ and $S_\downarrow$ with approximately the same absolute value ($\sim 12\,\mu$V/K) and opposite signs, meaning that the thermally induced voltages generated at a given temperature difference will drive the electrons with opposite spins in contrary directions. In the range $V_g = 0.1 - 0.4$ V, $S_\uparrow$ shows a nearly constant behavior, decreasing very slowly, from $-14.2\,\mu$V/K at $V_g = 1$ V to $-15.6\,\mu$V/K at $V_g = 4$ V. Conversely, $S_\downarrow$ shows a parabolic shape, varying around zero with small magnitude values. Thus, in this range of gate voltages, the system is in a regime presenting $|S_\uparrow| \approx 14 - 15\,\mu$V/K and $S_\downarrow \sim 0$. On the other hand, as V_g decreases to negative values, $S_\uparrow$ grows steadily from a negative value of $-11.8\,\mu$V/K at $V_g = 0$ V to a positive one, $+3.6\,\mu$V/K at $V_g = -4$ V, crossing zero at a gate voltage close to $V_g = -3$ V; $S_\downarrow$ grows faster and shows a peak around $V_g = -2.5$ V, where $S_\downarrow = 83.2\,\mu$V/K and $S_\uparrow = -1.9\,\mu$V/K. Then, close to the peak maximum, where S_{tot} and $S_\downarrow$ intersect, the system presents high $S_\downarrow$ and negligible $S_\uparrow$. Therefore, we identify three distinct regimes into which the present device can be tuned: (i) negligible $S_\uparrow$ and high positive $S_\downarrow$ (at negative V_g); (ii) $S_\uparrow \sim -S_\downarrow$, close to zero V_g; and (iii) negative $S_\uparrow$ and negligible $S_\downarrow$ (at positive V_g).

To further characterize our device, we calculated the current (Eq. 1) as a function of the gate voltage for a fixed temperature difference of 30 K between the left and right electrodes (fixing $T_L = 300$ K and $T_R = 330$ K) while keeping the external bias voltage at zero. The results, plotted in Fig. 3, show more clearly how the current varies as V_g changes, passing through the three distinct regimes discussed. For the current, which can be approximated by $I_\sigma = -G_\sigma S_\sigma \Delta T$, where G_σ is the conductance, for small ΔT; the values or ranges of gate voltages at which every regime happens can be somewhat different when comparing to S due to the dependence of the current on the conductance as well. However, the behavior of the currents resembles that of the Seebeck coefficient. Regime (i) ($I_\uparrow \sim 0$ and high $I_\downarrow$) occurs in a narrower range around $V_g = -2.5$ V due to the faster increase of $I_\downarrow$ with decreasing V_g. Regime (iii) (negative $I_\uparrow$ and $I_\downarrow \sim 0$) happens in the range $V_g = 2 - 4$ V and

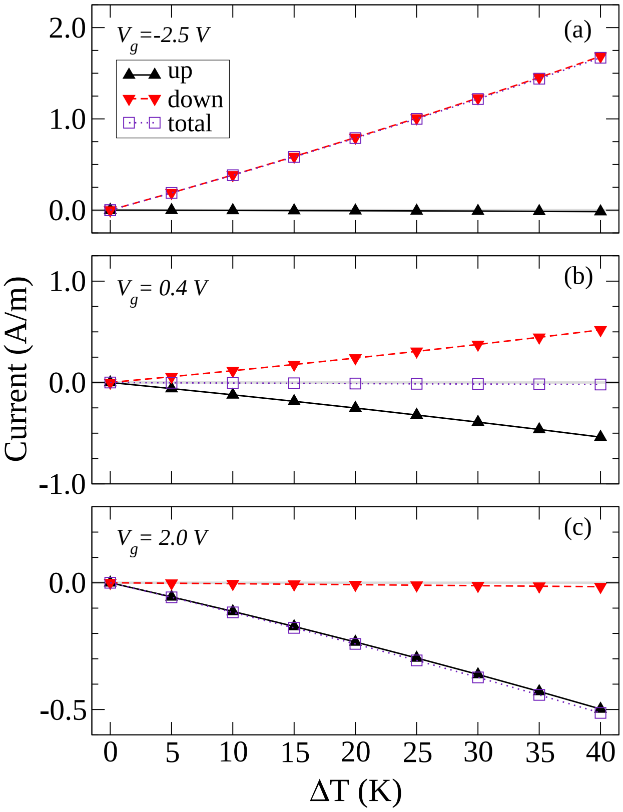

FIG. 4. (Color online) Current versus temperature difference ($T_L = 300$ K and $T_R = T_L + \Delta T$) for the applied gate voltages of $V_g = -2.5$ V, 0.4 V and 2.0 V, from (a) to (c) respectively. Notice the different scales for the current. The lines are just guides to the eyes.

regime (ii), at which there is no net charge transport ($I_\uparrow = -I_\uparrow$), at $V_g = 0.4$ V, presenting a slight shift from the value of $V_g = 0.24$ V for the Seebeck coefficient.

The behavior of the current at different temperature differences for the gate voltages $V_g = -2.5$, 0.4 and 2.0 V, which are representative of each regime described above, (i) to (iii) respectively, is shown in Fig. 4 for a fixed $T_L = 300$ K and varying the temperature of the right contact as $T_R = T_L + \Delta T$. As can be seen in the figure, the currents follow a linear trend with ΔT, indicating that the system is in the linear transport regime. For $V_g = -2.5$ V, when the device is in regime (i) (see Fig. 4a), $I_\uparrow \approx 0$ A/m in all the calculated range of temperatures whereas $I_\downarrow$ reaches up to 1.69 A/m at $\Delta T = 40$ K. Then in this case, the total current, $I_{tot} = I_\uparrow + I_\downarrow$, consists practically of down-spin electrons only, and has a charge polarization, given by $(|I_\uparrow| - |I_\downarrow|)/(|I_\uparrow| + |I_\downarrow|)$, of -98%. At $V_g = 0.4$ V the system is in regime (ii) (Fig. 4b), where for all the calculated ΔTs, the currents for both spins are similar in magnitude (~ 0.52 A/m at $\Delta T = 40$ K) but have opposite directions (given by the sign of the currents). The up- and down-spin currents cancel each other out and I_{tot} is then negligible. Thus, the device displays counter-propagating spin currents without any net charge transport. At $V_g = 2.0$ V the system reaches regime (iii), showing a behavior opposite to (i). The down-spin current is almost negligible, $I_\downarrow \approx 0$, in all the temperature range calculated and $I_\uparrow$ attains -0.50 A/m for $\Delta T = 40$ K. The total current is then basically made of up-electrons only, $I_{tot} \approx I_\uparrow$, and shows a charge polarization as high as 94%.

It is important to note that our proposed device is quite small and that a more realistic one would have a larger area with Mn randomly distributed over it, and possibly trapped at different types of defects other than only single vacancies. However, if the defects are created by ion bombardment, for example, the predominance of the type of defects can be adjusted by the beam energy[28,29]. Also, anti-ferromagnetic coupling among neighboring Mn should be prevented. This could be avoided either by keeping a low enough density of Mn@SV or by aligning the Mn local magnetic moments using a magnetic field (or both). Under these conditions, the effect of disorder in the distribution of defects may lead the system into a localized regime at which the spin asymmetry of transport properties, the Seebeck effect included, could be enhanced[30,31]. Other point worth considering is the use of other metals as dopants (such as Fe, Ni, Co or Au and Ag). In principle, any metal showing spin-dependent transmittance close to the Fermi level may present spin-dependent Seebeck effect (see Eq. 2). Finally, the effects of the presence of different substrates should be taken into account when building the real device. Depending on the substrate, graphene may be p- or n-type doped already and then, the gate voltages needed to attain the different regimes will be somewhat different. Yet, the overall picture for the device will still be the same. Local substrate doping can also be used as a substitute for the effect of the gate potential, raising or lowering the energy levels of the region containing the Mn atoms.

In summary, we have proposed a proof-of-concept device made of graphene with Mn atoms trapped in single vacancies showing a highly tunable spin dependent Seebeck effect, which could open a new door for applications of graphene in spin caloritronics.

ACKNOWLEDGMENTS

We would like to thank A. R. Rocha for a critical reading of the manuscript and useful suggestions. This work has received financial support from the brazilian agencies CNPq, INCT-Nanomateriais de Carbono and FAPESP. The calculations have been performed in the GPU cluster at CENAPAD-SP.

[1] G. E. W. Bauer, E. Saitoh, and B. J. van Wees, Nature Mater. **11**, 391 (2012).
[2] K. S. Novoselov, A. K. Geim, S. V. Morozov, D. Jiang, Y. Zhang, S. V. Dubonos, I. V. Grigorieva, and A. A. Firsov, Science **306**, 666 (2004).
[3] A. H. Castro Neto, F. Guinea, N. M. R. Peres, K. S. Novoselov, and A. K. Geim, Rev. Mod. Phys. **81**, 109 (2009).

[4] V. M. Karpan, G. Giovannetti, P. A. Khomyakov, M. Talanana, A. A. Starikov, M. Zwierzycki, J. van den Brink, G. Brocks, and P. J. Kelly, Phys. Rev. Lett. **99**, 176602 (2007).

[5] N. Tombros, C. Jozsa, M. Popinciuc, H. T. Jonkman, and B. J. van Wees, Nature **448**, 571 (2007).

[6] D. Dragoman and M. Dragoman, Appl. Phys. Lett. **91**, 203116 (2007).

[7] B. Zhou, B. Zhou, Z. Liu, and G. Zhou, J. Appl. Phys. **112**, 073712 (2012).

[8] Y. M. Zuev, W. Chang, and P. Kim, Phys. Rev. Lett. **102**, 096807 (2009).

[9] D. Basko, Science **334**, 610 (2011).

[10] X. Wu, Y. Hu, M. Ruan, N. K. Madiomanana, C. Berger, and W. A. de Heer, Appl. Phys. Lett. **99**, 133102 (2011).

[11] M. Zeng, Y. Feng, and G. Liang, Nano Lett. **11**, 1369 (2011).

[12] M. Zeng, Y. Feng, and G. Liang, Applied Physics Letters **99**, 123114 (2011).

[13] F. Schwierz, Nature Nanotech. **5**, 487 (2010).

[14] O. Cretu, A. V. Krasheninnikov, J. A. Rodríguez-Manzo, L. Sun, R. M. Nieminen, and F. Banhart, Phys. Rev. Lett. **105**, 196102 (2010).

[15] M. P. Lima, A. J. R. da Silva, and A. Fazzio, Phys. Rev. B **84**, 245411 (2011).

[16] E. J. G. Santos, A. Ayuela, and D. Sánchez-Portal, New J. Phys. **12**, 053012 (2010).

[17] C. Cao, M. Wu, J. Jiang, and H.-P. Cheng, Phys. Rev. B **81**, 205424 (2010).

[18] E. J. G. Santos, D. Sánchez-Portal, and A. Ayuela, Phys. Rev. B **81**, 125433 (2010).

[19] A. V. Krasheninnikov, P. O. Lehtinen, A. S. Foster, P. Pyykkö, and R. M. Nieminen, Phys. Rev. Lett. **102**, 126807 (2009).

[20] Y. Tang, Z. Yang, and X. Dai, J. Chem. Phys. **135**, 224704 (2011).

[21] E. Artacho, D. Sánchez-Portal, P. Ordejón, A. García, and J. M. Soler, Phys. Status Solidi (b) **215**, 809 (1999).

[22] F. D. Novaes, A. J. R. da Silva, and A. Fazzio, Braz. J. Phys. **36**, 799 (2006); J. E. Padilha, M. P. Lima, A. J. R. da Silva, and A. Fazzio, Phys. Rev. B **84**, 113412 (2011); The code has been modified to allow the use of graphical processing units (GPUs).

[23] J. P. Perdew, K. Burke, and M. Ernzerhof, Phys. Rev. Lett. **77**, 3865 (1996).

[24] N. Troullier and J. L. Martins, Phys. Rev. B **43**, 1993 (1991).

[25] H. J. Monkhorst and J. D. Pack, Phys. Rev. B **13**, 5188 (1976).

[26] R. Landauer, Philos. Mag. **21**, 863 (1970); M. Büttiker, Y. Imry, R. Landauer, and S. Pinhas, Phys. Rev. B **31**, 6207 (1985); M. Büttiker, Phys. Rev. Lett. **57**, 1761 (1986).

[27] U. Sivan and Y. Imry, Phys. Rev. B **33**, 551 (1986).

[28] A. W. Robertson, B. Montanari, K. He, J. Kim, C. S. Allen, Y. A. Wu, J. Olivier, J. Neethling, N. Harrison, A. I. Kirkland, and J. H. Warner, Nano Letters **13**, 1468 (2013).

[29] A. W. Robertson, C. S. Allen, Y. A. Wu, K. He, J. Olivier, J. Neethling, A. I. Kirkland, and J. H. Warner, Nature Communications **3** (2012), 10.1038/ncomms2141.

[30] A. R. Rocha, T. B. Martins, A. Fazzio, and A. J. R. da Silva, Nanotechnology **21**, 345202 (2010).

[31] J. M. de Almeida, A. R. Rocha, A. J. R. da Silva, and A. Fazzio, Phys. Rev. B **84**, 085412 (2011).